



Combined Synchrotron X-ray and Neutron Powder Diffraction Studies of $\text{Ba}_2\text{InSbO}_6$ Ordered Double Perovskite

R. Shaheen, J. Bashir*, M.N. Khan and K. Shahzad

Physics Division, Directorate of Science, PINSTECH, P. O. Nilore, Islamabad, Pakistan

(Received September 05, 2014 and accepted in revised form September 25, 2014)

The crystal structure of $\text{Ba}_2\text{InSbO}_6$, prepared via solid state reaction, has been investigated by powder neutron and Synchrotron X-ray, diffraction techniques. From the detailed analysis of the diffraction patterns, it was shown that the crystal structure can be best described by the high-symmetry cubic doubled perovskite cell, space group $\text{Fm}\bar{3}\text{m}$, with cell parameters $a = 8.2639(1) \text{ \AA}$. The structure was found to be stable down to 100K making it a suitable candidate for growing thin films of high temperature superconductors.

Keywords : Synchrotron X-ray diffraction, Double perovskite, Antimony based ordered perovskite, Rietveld refinement

1. Introduction

Owing to their interesting magnetic properties and possibility of using these materials as substrate for growing thin films of high T_c superconductors, antimony based double perovskites have aroused a great deal of interest [1-8]

Previously, the crystal structure of $\text{Ba}_2\text{InSbO}_6$ (BISO) is reported either being disordered aristotype (space group $\text{Pm}\bar{3}\text{m}$) or ordered elpasolites (space group $\text{Fm}\bar{3}\text{m}$) [2, 5, 9-11]. These variations about the crystal structure of BISO reported in literature can be explained by the fact that scattering powers of both In and Sb ions are quite similar, making it difficult to observe the weak superstructure reflections arising from the rock salt ordering of BB' cations and the tilting of octahedra. At the same time, laboratory X-ray diffractometers possess low resolution making it difficult to examine the peak splitting. Furthermore, from X-ray diffraction measurements, it is difficult to locate lighter atoms such as oxygen. All these problems can be overcome either by the use of neutron powder diffraction or Synchrotron X-ray diffraction techniques. With neutron powder diffraction, location of lighter elements such as oxygen becomes easier whereas high brilliance and resolution of Synchrotron sources make it possible to observe the weak superstructure reflections and peak splitting patterns. In our earlier study, with prolong counting time, in conventional lab X-ray diffractometer; we were able to show that the structure of BISO is indeed ordered [12]. However, no peaks splitting were observed, owing to the limited resolution of the laboratory X-ray diffractometers, the results were therefore a bit inconclusive about the true space group

of BISO. In this paper, we now report the results of neutron diffraction and Synchrotron X-ray diffraction measurements to further confirm the assigned space group. Consequently also explored the possible structural phase transformation by if BISO is to be used as substrates for growing thin films of high T_c superconductors, it is essential to study its structure stability by lower temperature dependent Synchrotron X-ray diffraction measurements.

2. Experimental

Polycrystalline sample of $\text{Ba}_2\text{InSbO}_6$ was prepared through standard solid-state reaction as described in our earlier work [12]. Room temperature powder neutron diffraction data was measured on High Resolution Powder Diffractometer (HRPD) at HANARO Center, KAERI with neutron wavelength of 1.839Å. HRPD is equipped with array of 32 detectors and the available scattering angle is up to 160.

High resolution Synchrotron X-ray diffraction studies were carried out at the MCX beam line, ELETTRA Sincrotrone, Trieste, Italy. The optics of the MCX beam line consists of two mirrors and a monochromator: the first Pt-coated cylindrical mirror collimates the beam on the horizontally focusing Si (111) double crystal monochromator in 1:1 configuration. The second - vertical focusing - platinum coated mirror is flat and bendable, with a radius adjustable from 6 km to flat. The double crystal monochromator (DCM) consists of two Si crystals (active area $50 \times 50 \text{ mm}^2$, manufactured cut along the [111] direction. Two successive Bragg reflections with an inherent energy resolution of 0.014% direct photons of the desired energy parallel to the incoming beam

* Corresponding author : javaid_bashir@yahoo.com

direction, but offset upward (out of the direct Bremsstrahlung beam). The second crystal provides Sagittal focusing; it is a ribbed crystal, cylindrically bent to a variable curvature radius [13].

The sample was packed in a quartz capillary of 0.3mm diameter and the diffraction patterns in $5 \leq 2\theta \leq 60^\circ$ range were collected with step size of 0.01° . In order to resolve the peak splitting, some peaks were measured with a step size of 0.005° . In order to avoid preferred orientation, the capillary was rotated during the course of experiments. For better compromise between reduction of absorption effect in the capillary and the necessity in high resolution to reveal peak splitting, the energy of the beam was set to 18KeV ($\lambda = 0.689 \text{ \AA}$). Low temperature measurements in $100\text{K} \leq T \leq 300\text{K}$ range were carried out with a blower from Oxford instruments.

Both neutron and Synchrotron X-ray powder diffraction data were analyzed by Rietveld profile analysis technique using programme Rietica [14]. Peak shapes were described by pseudo-Voigt function with peak asymmetry corrections and background was fitted by a fourth order polynomial. The refined parameters were background coefficients, scale factors, lattice constants, atomic positions and individual thermal parameters as well as the usual profile parameters describing the pseudo-Voigt peaks shape function. Anti-site defect concentrations were determined by allowing the occupancies of In and Sb ions in their respective positions to be varied with the constraints that (a) the overall stoichiometry remains as $\text{Ba}_2\text{InSbO}_6$ and (b) the octahedral sites remain fully occupied.

3. Results and Discussion

Having established earlier that the crystal structure of BISO is ordered [12], we have tried various models which permit the rock salt ordering of the BB' cations over the six coordinated octahedral sites such as cubic ($Fm\bar{3}m$), monoclinic ($P2_1/n$ and $I2/m$) and tetragonal ($I4/m$). Model parameters such as lattice constants and fractional atomic coordinates were either taken from Shaheen & Bashir [12] or were generated by SPuDs [15].

From the reliability parameters listed in Table 1, as obtained from the Rietveld model fitting to the neutron diffraction data, it is obvious that all four structural models fit the neutron diffraction data well. Though Rietveld fitting (Figure 1) based on monoclinic (space group $P2_1/n$) yielded the lowest values of R_p (3.77%) and χ^2 (2.86), however, the spread in the reliability parameters for various models is quite small making it difficult to assign the correct space group.

Table 1. Rietveld Reliability parameters for various models obtained from the neutron diffraction data.

Space group	Reliability Parameters	
	R_p (%)	χ^2
$P2_1/n$	3.77	2.86
$Fm\bar{3}m$	3.98	3.18
$I2/m$	4.03	3.29
$I4/m$	4.11	3.84

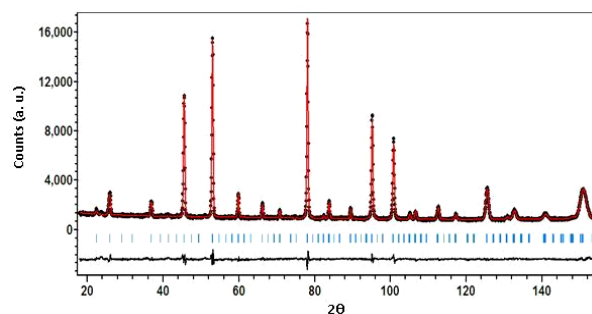


Figure 1. Rietveld fitting of the neutron diffraction data based on the monoclinic structure (space group $P2_1/n$). Filled circles are the observed intensity data, red line is calculated intensity, and vertical bars at the bottom are reflection positions based on monoclinic symmetry. Black continuous line at the bottom depicts difference between the observed and the calculated intensities.

One way of assigning the space group is by examining the reflections arising from the tilting of the octahedra. Presence of *even-odd-odd* (*eoo*) and *odd-odd-odd* (*ooo*) superstructure reflections in the diffraction pattern indicates in-phase tilting and out of phase tilting of the octahedra and/or by the rock salt ordering of the BB' cations respectively. Simultaneous presence of in-phase and out of phase tilting will produce *even-odd-odd* (*eoo*) reflections. In Figure 2, enlarged section of the neutron diffraction pattern fitted with two models is shown. The upper vertical bars, indicating position of possible reflections, shown at the bottom of the diffraction pattern correspond to model based on monoclinic symmetry (space group $P2_1/n$) whereas the lower vertical bars correspond to the cubic model (space group $Fm\bar{3}m$). The indexing of reflections is for space group $Fm\bar{3}m$. It is clear from Figure 2 that no reflections indicative of in-phase or out of phase tilting, indicated by *, are present in the neutron diffraction pattern. Furthermore, close inspection of (220), (420) and (422) reflections do not reveal any splitting. If the structure would have been monoclinic, (220), (420) and (422) reflections would split in 1:4:1, 1:2:2:1 and 2:1:1:2 manner respectively, and if these reflections split in 2:1, 1:1:1 and 1:2 manner then the structure would have been tetragonal. Similarly, neither the reflections arising from the tilting of the octahedral nor the peak splitting was observed in the Synchrotron

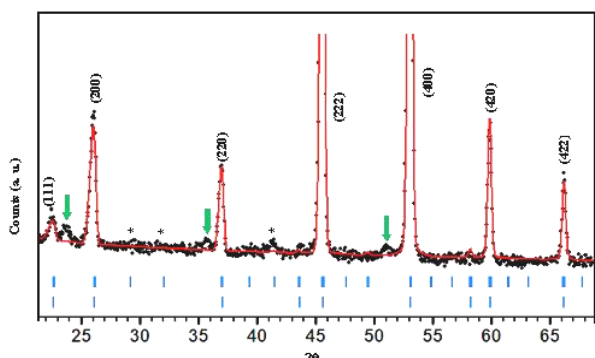


Figure 2. Enlarged portion of neutron diffraction pattern fitted with monoclinic model (space group $P2_1/n$). * indicates reflections indicative of in-phase and out of phase tilting of the octahedral. Vertical bars at the bottom of the graph indicate possible peak positions in the two space groups. Arrows indicate unidentified impurity. However, this impurity phase was not visible in Synchrotron X-ray diffraction patterns. Since the intensities of impurity phase were quite low, it was not possible to identify. Considering that impurity phase is not visible in Synchrotron X-ray diffraction patterns, it is hypothesized that it may be coming from the diffraction of neutrons from some component in the neutron diffractometer.

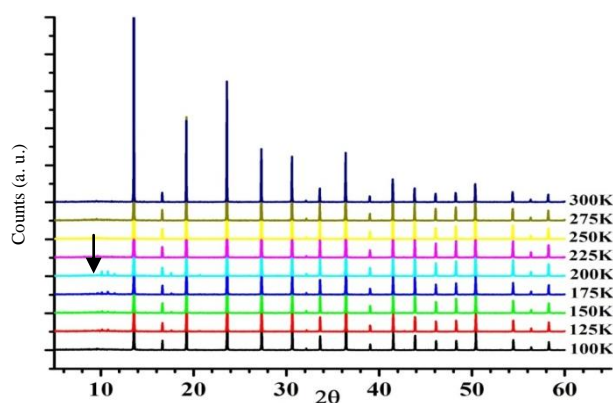


Figure 3. Synchrotron X-ray diffraction patterns measured at different temperatures. Arrows indicate reflections due to deposition of ice on the surface of the capillaries during the low temperature measurements.

X-ray diffraction patterns as shown in Figure 3 and Figure 4. As an example, (422) reflection measured with a step size of 0.005° is shown in the inset of Figure 4 which clearly indicates absence of any peak splitting. Consequently, on the basis of these arguments, it is safe to conclude that the space group is $Fm\bar{3}m$ and not $P2_1/n$.

The results of simultaneous refinement of room temperature Synchrotron and neutron diffraction data are given in Table 1. The measured lattice constant, $a = 8.2621(1) \text{ \AA}$ and In – O and Sb – O bond distances ($r_{\text{In-O}} = 2.1582(1) \text{ \AA}$ and $r_{\text{Sb-O}} = 1.9852(1) \text{ \AA}$ are in

good agreement with earlier reported results [12]. In the present investigations, we were unable to find any anti-site disorder in contrast without previously reported results

Table 2. Refined structural parameters at room temperature as obtained from the combined refinement of neutron and Synchrotron X-ray diffraction data.

Atom	χ	y	z	$B_{\text{iso}}(\text{\AA}^2)$	N
Ba	$\frac{1}{4}$	$\frac{1}{4}$	$\frac{1}{4}$	0.55(3)	1
In	0	0	0	0.12(8)	1
Sb	$\frac{1}{2}$	0	0	0.50(3)	1
O	0.2601(1)	0	0	0.58(3)	1

The Synchrotron X-ray diffraction patterns measured at various temperatures are shown in Figure 3 whereas fitted diffraction data based on $Fm\bar{3}m$ model is shown in Figure 4. No change in the diffraction pattern is observed as a function of temperature indicating that the structure is stable down to 100K making it suitable substrate for growing thin films of high T_c superconductors. The lattice constant decreases linearly with temperature. The bond distances also show variation with temperature. The oxygen positional parameter x_O , stays constant in the entire temperature range of investigation. and the temperature dependence of overall temperature factor, B_{overall} is quite weak (Table 3).

Table 3. Refined structural parameters and reliability parameters as obtained from model fitting to the Synchrotron X-ray diffraction data as a function of temperature. Owing to the tendency of individual temperature factors becoming negative, only the overall temperature factors were refined.

T (K)	a(A)	x_O	$B_{\text{overall}}(\text{\AA}^2)$	χ^2	$R_{\text{Bragg}}(\%)$
300	8.2591 (1)	0.235(2)	0.62(2)	1.58	2.08
275	8.2571 (1)	0.238(2)	0.59(2)	1.55	4.36
250	8.2558 (1)	0.235(1)	0.54(2)	1.58	3.17
225	8.2537 (1)	0.236(1)	0.32(2)	1.55	3.90
200	8.2523 (1)	0.236(2)	0.02(2)	1.88	3.78
175	8.2514 (1)	0.236(2)	0.45(2)	1.75	4.66
150	8.2499 (1)	0.235(2)	0.28(2)	1.60	3.95
125	8.2488 (1)	0.236(2)	0.41(3)	1.66	5.37
100	8.2477 (1)	0.236(2)	0.41(2)	1.88	4.21

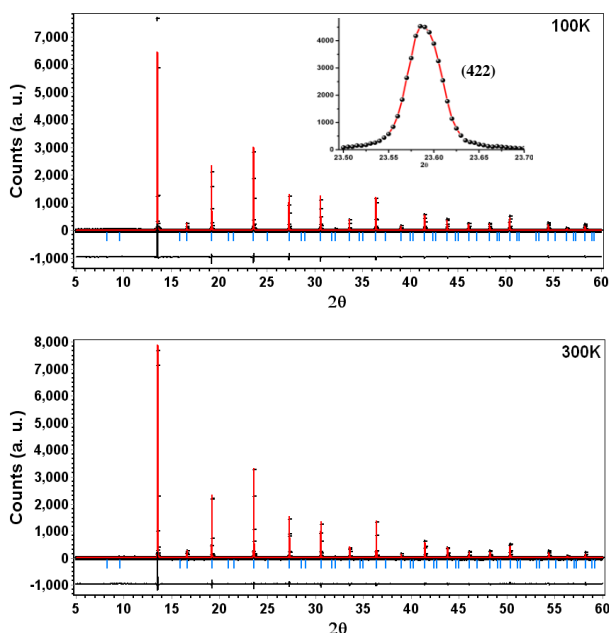


Figure 4. Fitted Synchrotron X-ray diffraction patterns at 300K and 100K. No peak splitting was observed in any of the diffraction patterns as is shown in the inset (422) reflection measured with step size of 0.005°.

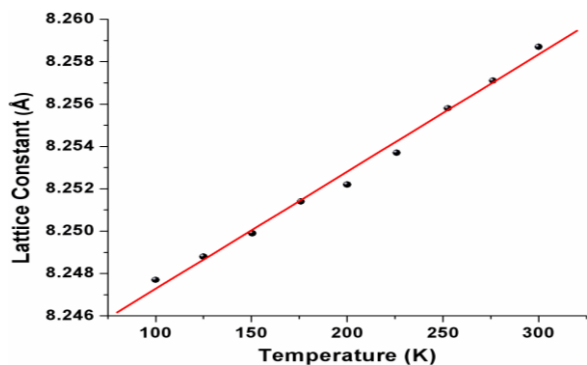


Figure 5. Temperature dependence of the lattice constant as a function of temperature.

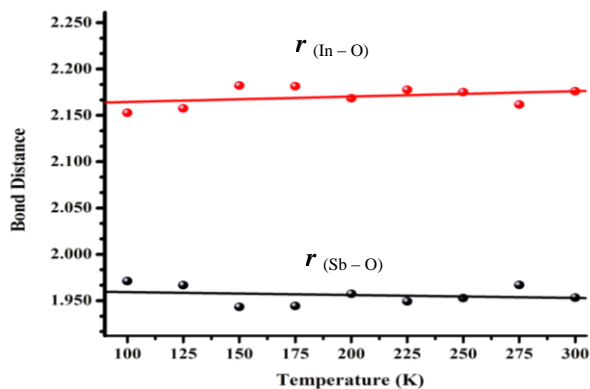


Figure 6. Temperature dependence of the inter-atomic distances as a function of temperature.

4. Conclusions

Both neutron diffraction and synchrotron X-ray diffraction techniques have been employed to investigate the crystal structure of BISO. Though values of reliability factors as obtained from fitting of neutron diffraction data indicate the structure to be monoclinic, however examination of superstructure reflections indicates that the structure is cubic. This is further confirmed by synchrotron X-ray diffraction measurements. No structural phase transformations were observed down to 100 K indicating the structural stability in the 100 – 300K temperature range making it a suitable candidate for growing thin films of high temperature superconductors.

Acknowledgements

The authors gratefully acknowledge staff at Central Diagnostic Laboratory for providing access to materials synthesis and X-ray diffraction facilities. The authors are also grateful to the ICTP – ELETTRA users programme for financial assistance for the execution of the project (Project ID 20110345). The authors gratefully acknowledge the help of Dr. Andrea LAUSI and Dr. Jasper Rikkert PLAISIER during the course of experiments at MCX beam line at ELETTRA. We are also indebted to Dr. Lee Chang-Hee for providing neutron diffraction data.

References

- [1] G. Blasse, *J. Appl. Phys.* **36** (1965) 879.
- [2] S.C. Tauber, R.D. Tidrow and W.D. Finnegan, *Physica C* **256** (1996) 340.
- [3] E.J. Cussen, J.F. Vente, P.D. Battle and T.C. Gibb, *J. Mater. Chem.* **7** (1997) 459.
- [4] N. Kashima, K. Inoue, T. Wada and Y. Yamaguchi, *Appl. Phys. A* **74** (2002) S805.
- [5] A.E. Lavat and E.J. Baran, *Vibrational Spectros.* **32** (2003) 167.
- [6] P. J. Saines and B. J. Kennedy, *J. of Solid State Chem.* **181** (2008) 298.
- [7] C. Bharti and T.P. Sinha, *Solid State Sci.* **12** (2010) 498.
- [8] A. Faik, D. Orobengoa, E. Iturbe-Zabalo and J.M. Igartua, *J. Solid State Chem.* **192** (2012) 273.
- [9] A.W. Sleight and R. Ward, *Inorg. Chem.* **3** (1964) 292.
- [10] V.V. Wittman, G. Rauser and S. Kimmier-Sack, *Z. Anorg. Allg. Chem.* **482** (1981) 143.
- [11] X.Y. Mei, L.J. Bie, C.H. Ma, H.B. Huang, R.H. Liu, W.J. Zheng and Y.F. Xia, *Chinese J. Inorg. Chem.* **24** (2008) 218.
- [12] R. Shaheen and J. Bashir, *Solid State Sci.* **12** (2010) 605.
- [13] A. Lausi, E. Busetto, M. Leoni and P. Scardi, *Synchrotron Radiation in Natural Science* **5** (2006) 1.
- [14] C.J. Howard and B.A. Hunter, *A Computer Programme for Rietveld Analysis of X-ray and Neutron Powder Diffraction Patterns*. Lucas Heights Research Laboratories, NSW, Australia (1998) pp. 1-27.
- [15] M.W. Lufaso, R.B. Macquart, Y. Lee, T. Vogt and Hans-Conrad zur Loye, *J. Solid State Chem.* **179** (2006) 91.